

## Contents of this file

- Text S1 to S2
- Figs. S1 to S6
- Caption for Dataset S1 ( dataset file ds01.csv uploaded separately)

## Introduction

Text S1 describes the estimations of the size distribution of the saltating particles, saltation mass flux, and saltation height based on the SPC-91 data. Text S2 describes the measurement uncertainties of the VREFM sensor. The E-field data measured in our field campaign are provided as a CSV file in Dataset S1. Additional figures (i.e., Figs. S1-S6) that support the findings of this study are also included.

\*Corresponding author: You-He Zhou, [zhouyh@lzu.edu.cn](mailto:zhouyh@lzu.edu.cn)

## Text S1. Estimating the size distribution of the saltating particles, saltation mass flux, and saltation height based on the SPC-91 data

Because SPC-91 sensors measure particle number passing through the measurement area ( $L_x=2$  mm in height and  $L_y=25$  mm in length) per second in the range of 30-490  $\mu\text{m}$  with 64 bins, the probability distribution function (PDF) of the saltating particle size can be readily estimated by

$$f(d < d_i < d + \Delta d) = \frac{N_i}{\Delta d \sum_{i=1}^n N_i} \quad (s1)$$

where  $f(d < d_i < d + \Delta d)$  denotes the probability density of particle size in the range of  $(d, d + \Delta d)$ ;  $N_i$  and  $d_i$  are the number and diameter of the  $i$ -th particle bin,

respectively. Examples of the PDF of the saltating particle size are shown in Fig. S1. It can be seen that the size of saltating particles at different heights nearly obeys a log-normal distribution (with  $R^2$  of 0.85-0.96).

In our field campaign, we measured the saltating particle number flux at 6 heights from 0.05 to 0.7 m. Thus, the mass flux at each measurement height can be reasonably estimated by

$$q(z) = \frac{\pi\rho_p}{6L_xL_yT_w} \sum_{i=1}^n (N_i d_i^3) \quad (\text{s2})$$

Note that the summation  $\sum$  is performed for the particles located in the range of  $[z, z + \Delta z]$  over the 30-min time windows (i.e.,  $T_w=30$  minutes), in order to collect sufficient sand samples and capture the full range of turbulent fluctuations (e.g. Martin and Kok, 2017; Sherman and Li, 2012). Since SPC-91 measures the particle diameter with an uncertainty of  $\Delta d = \pm 0.015$  mm (see SPC-91 Installation Guide, Niigata Electric Co., Ltd. for details), the uncertainty of estimating mass flux is  $\Delta q \sim 3d^2\Delta d$  (i.e.  $q \sim d^3 \Rightarrow \Delta q \sim 3d^2\Delta d$ ). As shown in Fig. S2, the measured mass flux data during different time intervals can be well fitted by the exponential functions (Shao, 2008):

$$q(z) = q_0 \exp(-az) \quad (\text{s3})$$

where  $q_0$  is the value of  $q$  at  $z = 0$  and  $a$  is a positive empirical constant. Hence, the total mass flux can be determined by

$$Q = \int_0^{+\infty} q(z) dz = \frac{q_0}{a} \quad (\text{s4})$$

Similarly, the uncertainty of the total mass flux is

$$\Delta Q = \frac{a\Delta q_0 - q_0\Delta a}{a^2} \quad (s5)$$

Additionally, the saltation height, which is defined as the height below which 99 % of the total mass flux is present, can be given by (Kok et al., 2012; Dupont et al., 2013)

$$\int_0^{z_{salt}} q(z)dz = \frac{0.99q_0}{a} \quad (s6a)$$

$$\Rightarrow z_{salt} = -\frac{\ln(0.01)}{a} \quad (s6b)$$

Similarly, the uncertainty of the saltation height is

$$\Delta z_{salt} = -\frac{\ln(0.01)}{a^2} \Delta a \quad (s7)$$

As shown in Fig. S3, the estimated saltation height slightly varies with time, and thus we use the mean saltation height, which is  $0.172 \pm 0.0343$  m, to obtain the dimensionless height  $z^*$ . For different time windows (i.e.  $T_w = 5, 10, 30$  minutes), there is no obvious differences between the mean values of  $Q$  and  $z_{salt}$ , but the standard deviations decrease as  $T_w$  increases (Fig. S3).

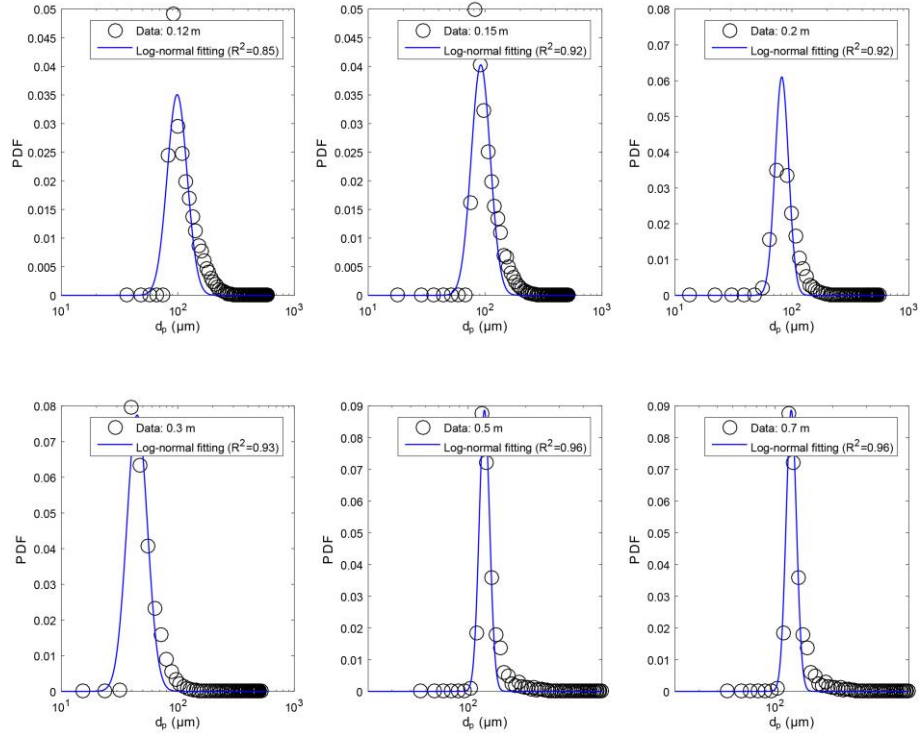
## Text S2. Measurement uncertainties of VREFM sensor

Fig. S4 shows the calibration results of three representative VREFM sensors. It can be seen that there is an excellent linear relationship ( $R^2=0.99-1$ ) between the output voltage of VREFM and the applied E-field intensities. The uncertainties of the VREFM sensor come primally from the fluctuation of the output voltage of VREFM sensors under a constant applied E-field, as shown in the left panels of Fig. S4. The uncertainties of a VREFM sensor under specific applied E-field can be defined as

$$\frac{k_{V-E} V'_{max}}{E_{applied}} \times 100\% \quad (s8)$$

where  $k_{V-E}$  is the slope of the fitting line in the right panels of Fig. S4;  $V'_{max}$  is the maximum fluctuation of the output voltage of VREFM sensors; and  $E_{applied}$  is the applied E-field intensity in the parallel-plate E-field calibrator. From the calibration results, we found that the maximum uncertainties of VREFM ranged from  $\sim 1.38\%$  to  $\sim 2.24\%$ .

**Dataset S1.** (ds01.csv) A CSV file contains 3-D E-field data measured in our field campaign from 12:30 to 18:30 on May 6, 2014, at the QLOA site. E1(1) to E1(5) represent the streamwise E-field at 0.05 to 0.7 m height, respectively; E2(1) to E2(5) represent the spanwise E-field at 0.05 to 0.7 m height, respectively; and E3(1) to E3(5) represent the vertical E-field at 0.05 to 0.7 m height, respectively. All data in the CSV file are shown in  $\text{kV m}^{-1}$ .



**Figure S1.** PDFs of the saltating particle size at different heights in the relatively stationary period of the observed dust storm (shown as the shaded area in Fig. 5 of the manuscript). Open squares denote measured data by SPC-91 sensors, and lines denote log-normal (i.e. Eq. 10 in the manuscript) fitting.

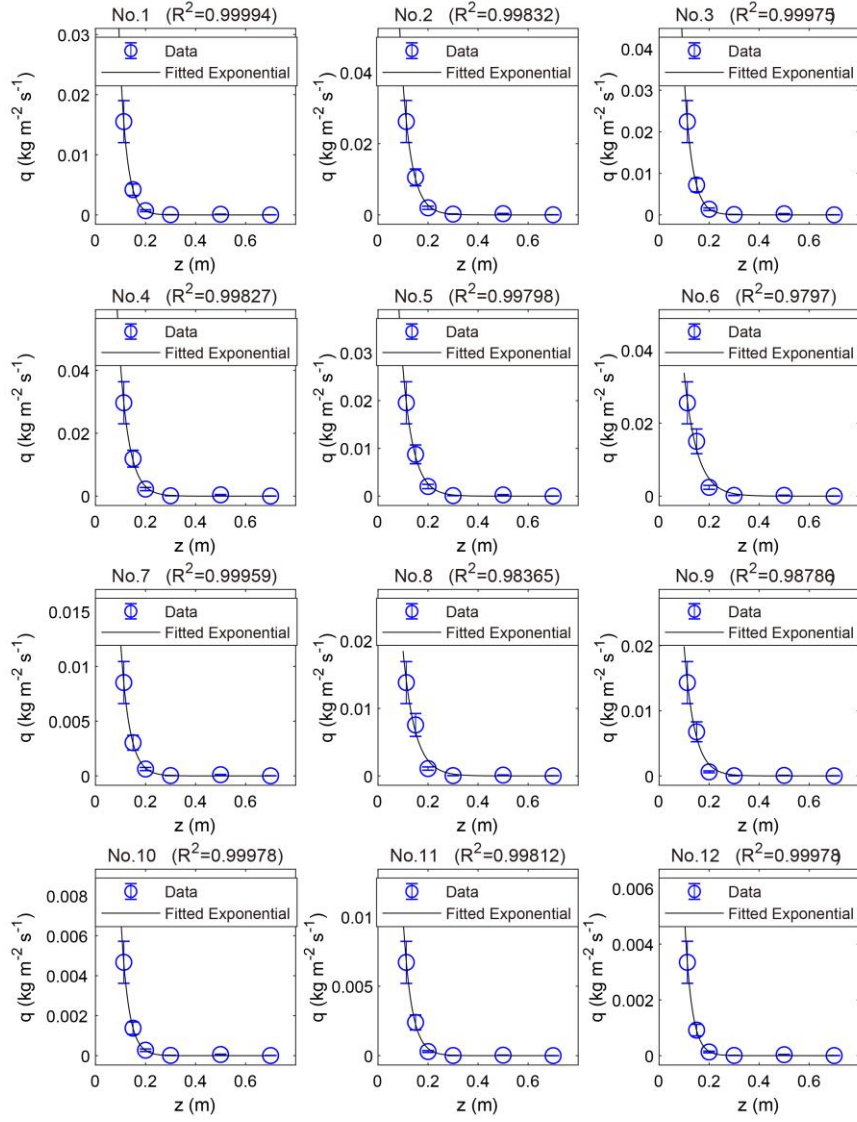


**Figure S2.** An example of the estimation of the total mass flux  $Q$  and saltation height  $z_{salt}$  in this study, where No.  $i$  corresponds to the time interval of  $[(i-1)T, iT]$ . The measured mass flux data are fitted by the exponential function  $q(z) = q_0 \exp(-az)$ , with  $R^2$  larger than 0.9. Thus, the total mass flux and saltation height can be estimated by Eqs. s4-s7 in the Supplement, respectively.

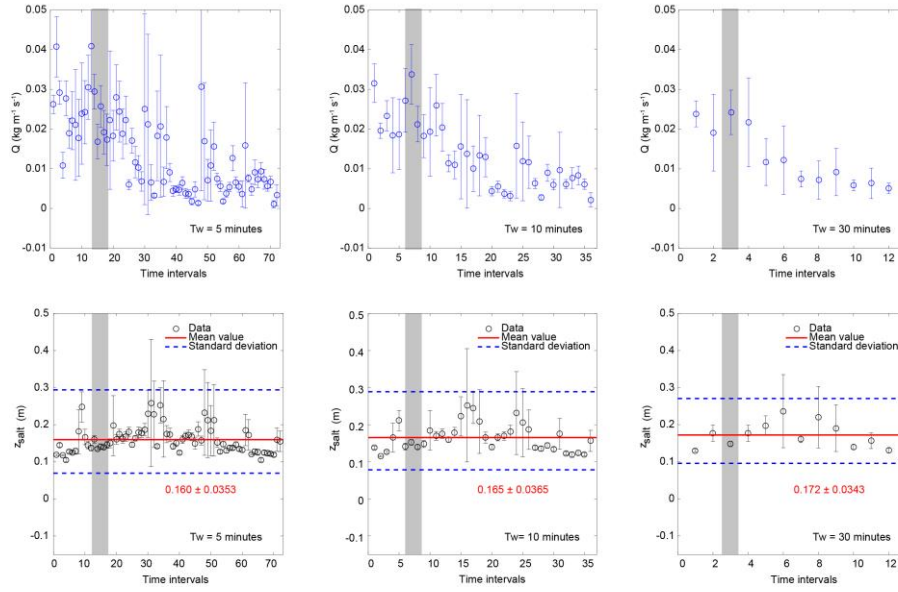


**Figure S3.** The estimated total mass flux  $Q$  (upper panels) and the saltation height  $z_{salt}$  (lower panels) with different time windows  $T_w$  (i.e. 5, 10, and 30 minutes) using the methods described in the Text S1. In the lower panels, the horizontal lines (in red) denote the mean saltation height, and the horizontal dashed lines (in blue) denote standard deviation. The shaded areas denote the relatively steady period of the observed dust storm.

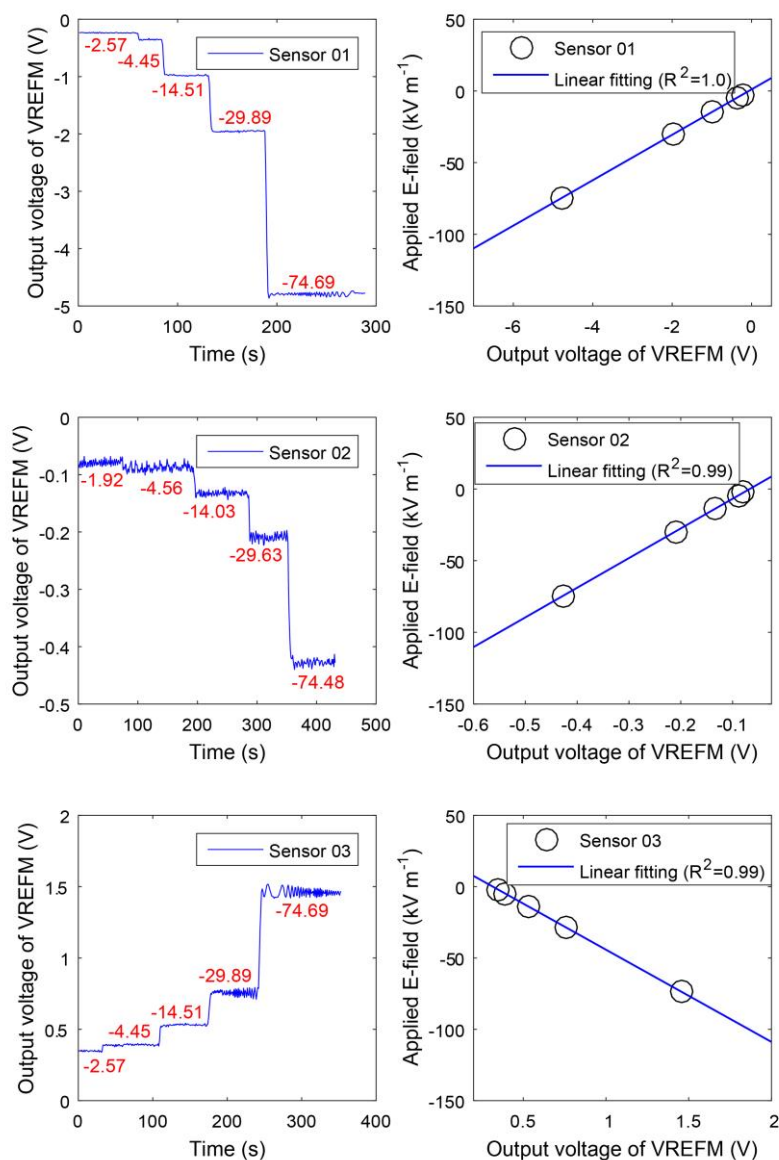


**Figure S4.** Examples of the calibration curves between the output voltage of the VREFM sensor and the applied E-field in the parallel-plate calibrator. The left panels are time series of the output voltage of the VREFM sensor at five different applied E-field levels (from  $\sim 2$  kV m<sup>-1</sup> to  $\sim 75$  kV m<sup>-1</sup> labeled in red). The right panels are the significant linear relationships between the output voltage of VREFM and the applied E-field intensity.



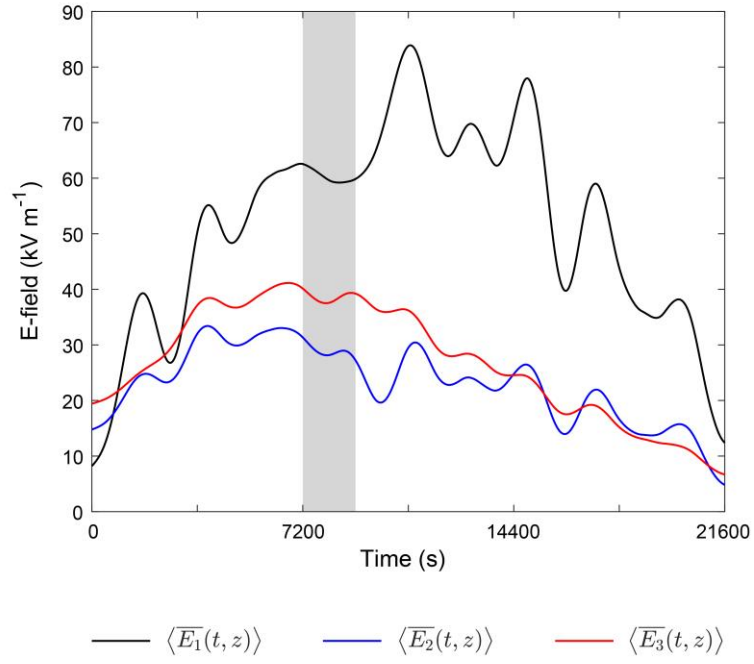


**Figure S5.** The height time-varying mean series of the 3-D E-field. The shaded area denotes the relatively steady period of the observed dust storms. Times are shown relative to May 6, 2014 at 13:00:00 UTC+8.

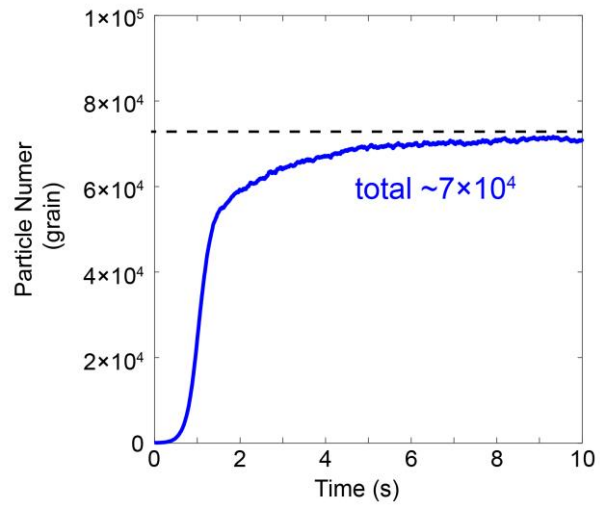


**Figure S6.** The total number of saltating particles in the case of Fig. 7 in the manuscript.

## References

- Dupont, S., Bergametti, G., Marticorena, B., and Simoens, S.: Modeling saltation intermittency, *J. Geophys. Res.-Atmos.*, 118, 7109–7128, doi:10.1002/jgrd.50528, 2013.
- Kok, J. F., Parteli, E. J., Michaels, T. I., and Karam, D. B.: The physics of wind-blown sand and dust, *Rep. Prog. Phys.*, 75, 106901, doi:10.1088/0034-4885/75/10/106901, 2012.
- Martin, R. L., and Kok, J. F.: Wind-invariant saltation heights imply linear scaling of aeolian saltation flux with shear stress, *Sci. adv.*, 3, doi: 10.1126/sciadv.1602569, 2017.
- Shao, Y. P.: *Physics and Modelling of Wind Erosion*, Springer Science & Business Media, Heidelberg, 2008.
- Sherman, D. J., and Li, B.: Predicting aeolian sand transport rates: A reevaluation of models, *Aeolian Res.*, 3, 371-378, doi: 10.1016/j.aeolia.2011.06.002, 2012.